

Crowding effect on helix-coil transition: beyond entropic stabilization

A. Koutsioubas,¹ D. Lairez,¹ S. Combet,¹ G. C. Fadda,^{1,2} S. Longeville,¹ and G. Zalczer³

¹⁾Laboratoire Léon Brillouin, CEA/CNRS UMR 12, CEA-Saclay, 91191 Gif-sur-Yvette cedex, France

²⁾Université Paris 13, UFR SMBH, 93017 Bobigny, France

³⁾Service de Physique de l'Etat Condensé, CEA-Saclay, 91191 Gif-sur-Yvette cedex, France.

(Dated: 20 June 2022)

We report circular dichroism measurements on the helix-coil transition of poly(L-glutamic acid) in solution with polyethylene glycol (PEG) as a crowding agent. Using small angle neutron scattering, PEG solutions have been characterized and found to be well described by the picture of a transient network of mesh size ξ , usual for semi-diluted chains in good solvent. We show that the increase of PEG concentration stabilizes the helices and increases the transition temperature. But more unexpectedly we also notice that the increase of crowding agent concentration reduces the mean helix extent at the transition, or in other words reduces its cooperative feature. This result cannot be accounted for by an entropic stabilization mechanism. Comparing the mean length of helices at the transition and the mesh size of the PEG network, our results strongly suggest two regimes: helices shorter or longer than the mesh size.

PACS numbers: 87.15.-v, 87.15.Cc, 87.15.hp

Proteins are the functional macromolecules of the cell. Their smooth functioning depends on a well determined three dimensional structure usually named as their "folded" state. The complete understanding of the way a linear polypeptide chain passes from a disordered and random coil conformation to this folded state, i.e. the protein folding process, is still puzzling and is a major challenge for current biology. In cells, macromolecule crowding and confinement play a central role in the thermodynamics of this folding process¹. The main idea lies in an "entropic stabilization mechanism": excluded volume due the presence of interface (confinement) or other macromolecules (crowding) lowers the conformational entropy of random conformations, which may favor the formation and the stabilization of well organized structures^{2,3}. In many cases, competition between different possible structures complicates the system and imposes to introduce refinements in order to account for the geometry and size of the confinement space or of the crowding agent⁴. Model and simplified systems are entry points to this complexity. In this context, α -helix that is one of the two main structural elements of proteins is particularly interesting, because helix-coil transition can be observed for homo-polypeptide. This allows us to get rid of the polyampholyte feature (presence in the same chain of positively and negatively charged monomers) and of the amphipathic feature (presence in the same chain of hydrophilic and hydrophobic monomers) of proteins. On the side of crowding effect studies, current trends for *in vitro* experiments use inert crowding agent such as Ficoll, a highly branched polysaccharide that behaves as compact and hard spheres, or polyethylene glycol (PEG) that behaves as a linear polymer in good solvent².

This paper is concerned with the helix-coil transition of poly(L-glutamic acid) chains embedded in a semi-dilute solution of PEG. We report circular dichroism measurements at different pH and PEG concentrations as a func-

tion of temperature. These measurements give access to the helix fraction x_h of a chain that can be considered as the order parameter of the transition. In contradiction with recent molecular dynamics simulations⁵, but in agreement with the entropic stabilization mechanism, we show that the helix-coil transition temperature T^* increases with PEG concentration. However, we show that unexpectedly the ratio T/T^* is not a reduced variable for x_h , i.e. the curves $x_h(T/T^*)$ obtained for the different PEG concentrations do not superimpose. In the framework of a transition between two states of different energy, this result firstly demonstrates the cooperativity of the helix formation, i.e. the necessity to introduce a coupling parameter in the free energy, and secondly that this feature depends on the PEG concentration.

The corollary of cooperativity is the existence of correlations in helix distribution. Traditionally, the first and simplest theoretical model introducing this ingredient is the Zimm-Bragg model⁶ that can be mapped into a one dimensional Ising model with an external field⁷ and an attractive (ferromagnetic) coupling between adjacent helix turns. By analyzing our data in this framework, we found that the attractive coupling becomes less efficient for increasing concentration of PEG. Our results suggest two regimes depending on the extent of helical domains compared to the mesh size of the PEG network.

I. RESULTS

A. Materials and methods

Poly(L-glutamic acid) ($M_w = 18$ kg/mol, polydispersity index 1.02) and polyethylene glycol ($M_w = 20$ kg/mol, polydispersity index 1.04) were purchased from Sigma Aldrich and were used without any further purification. Aqueous solutions (10 mM phosphate

buffer) containing various concentrations of PEG (up to 30 wt%) were vigorously agitated for at least two days in order to ensure complete dilution. The pH of the solutions was adjusted by addition of HCl and NaOH aqueous solutions. Before each measurement a small volume of relatively concentrated solution of poly(L-glutamic acid) was added in order to achieve a final peptide concentration of $10 \mu\text{M}$.

Small angle neutron scattering (SANS) measurements were performed with PACE spectrometer (LLB neutron facility) on PEG solutions in heavy water. Data reduction was done following ref.⁸.

Circular dichroism (CD) measurements were conducted using a JASCO J-815 CD spectrometer (CEA/DSV/iBiTec-S/SIMOPRO). Solutions were placed in quartz cuvettes with 1 mm path length. At the fixed wavelength of 222 nm, temperature scans in the range of 5-95°C (heating and cooling rates equal to 1 deg/min) were performed using a Peltier device.

B. SANS characterization of PEG solutions

PEG solutions have been first characterized by SANS measurements. Spectra are plotted for different volume fractions ϕ_{PEG} in Fig.1. They were fitted using a lorentzian shape following the Ornstein-Zernike approximation expected for linear polymer in semi-dilute solution⁹:

$$I(q) = \frac{I(0)}{1 + (q\xi)^2} \quad (1)$$

where I is the coherent differential scattering cross section per unit volume, $I(0)$ its value extrapolated at $q = 0$ and ξ the correlation length of concentration fluctuations. The corresponding mass, i.e. the mass of a chain segment of size ξ , is $m(\xi) = I(0)/K^2\phi_{\text{PEG}}$, where ϕ_{PEG} is the volume fraction of PEG and $K^2 = 4.3 \times 10^{-3} \text{ cm}^{-1} \text{ g}^{-1} \text{ mol}$ its contrast factor in heavy water. If a and m_a denote the size and the mass of the monomer, for a semi-dilute solution ξ/a and $g = m(\xi)/m_a$ can be interpreted as the mean short distance and the curvilinear distance between neighboring polymer chains⁹, both expressed in monomer unit. Results are plotted in Fig.2. We found $\xi/a = (1.10 \pm 0.02)\phi_{\text{PEG}}^{-0.75 \pm 0.03}$ and $g = (1.14 \pm 0.02)\phi_{\text{PEG}}^{-1.31 \pm 0.01}$ in very good agreement with the scaling laws for semi-dilute polymers in good solvent⁹.

C. Circular dichroism

Circular dichroism measurements have been performed on poly(L-glutamic acid) $10 \mu\text{M}$ aqueous solutions. We focused on the ellipticity θ per amino acid measured at 222 nm that allows us to deduce the fraction of amino acid of poly(L-glutamic acid) involved in α -helices. In Fig.3, the ellipticity measured as a function of temperature for heating rate equal to 1 deg/min is plotted for different

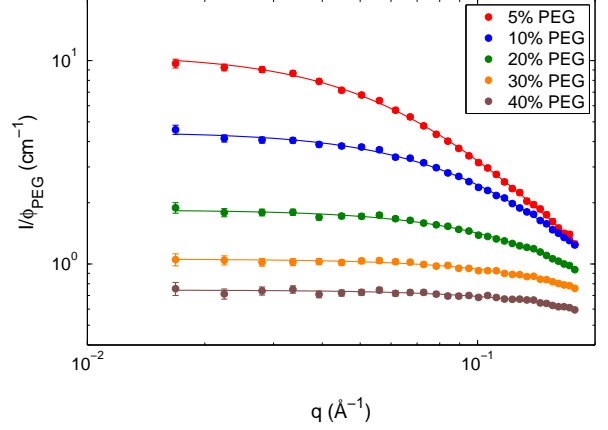


FIG. 1. Coherent differential scattering cross section per unit volume and unit of PEG volume fraction I/ϕ_{PEG} vs. scattering vector q for PEG solutions. Lines are best fits following Eq.1.

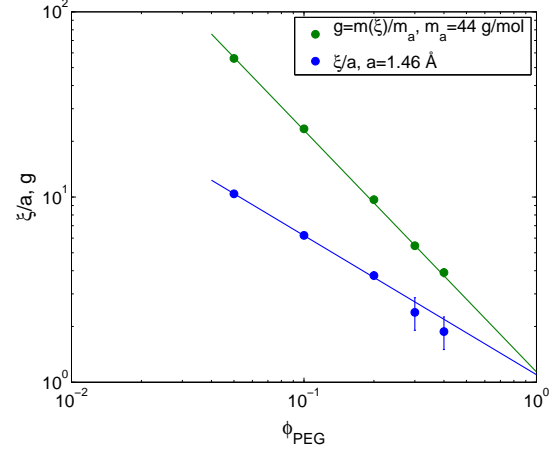


FIG. 2. Mean short distance, ξ/a , and curvilinear distance, $g = m(\xi)/m_a$, between neighboring PEG chains vs. PEG volume fraction ϕ_{PEG} , obtained from SANS data fitting using Eq.1, with m_a the molar mass of the monomer and a its length from ref.¹⁰. Straight lines are best power law fits corresponding to $\xi/a \propto \phi_{\text{PEG}}^{-0.75 \pm 0.03}$ and $g \propto \phi_{\text{PEG}}^{-1.31 \pm 0.01}$, respectively.

pH values. In this figure the horizontal dashed line indicates the value $\theta_{1/2} = \theta(T^*) = (\theta(0) - \theta(\infty))/2 + \theta(\infty)$ corresponding to the fraction 1/2 of helix amount at the transition temperature T^* . The asymptotic value $\theta(\infty)$ was estimated from our measurements as equal to $-3500 \text{ deg cm}^2 \text{ dmol}^{-1}$, whereas $\theta(0)$ (corresponding to 100% of helix) was taken as equal to $-3.7 \times 10^4 \text{ deg cm}^2 \text{ dmol}^{-1}$ according to ref.¹¹. The intercept of each experimental curve with this line allows us to determine the transition temperature T^* . The lower the ellipticity, the higher the helix amount, thus our measurements indicate clearly that for poly(L-glutamic acid) at a given temperature, the helix amount strongly decreases with

increasing pH values. Actually, increasing pH carboxylic acid groups are dissociated leading to electrostatic repulsions between amino acids and thus to an increase of the effective bond enthalpy H_B per amino acid involved in a helix. This yields to an increase of the transition temperature T^* ¹². In this work, we have taken advantage of this feature to finely tune T^* in the temperature window accessible for experiments at atmospheric pressure. In Fig.3, we can see that decreasing pH, the transition just enters in the accessible temperature window at pH=3.75, allowing possible further stabilization due to PEG to be studied. Note that at even smaller pH values, poly(L-glutamic acid) precipitates. In this regime, this experimental issue is clearly evidenced by heating and cooling measurements that do not superimpose.

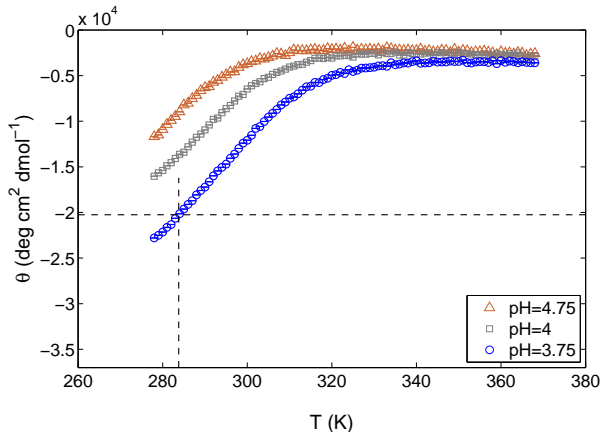


FIG. 3. Ellipticity θ at 222 nm per amino acid of poly(L-glutamic acid) solutions vs. temperature for different pH values. The horizontal dashed line has an ordinate $\theta_{1/2}$ corresponding to the helix fraction $1/2$. At even smaller pH, poly(L-glutamic acid) precipitates.

At pH=3.75, circular dichroism measurements have been performed as a function of temperature for different volume fractions of PEG. Results are plotted in Fig.4. Measurements indicate plainly the stabilization of helices with PEG addition. For heating and cooling rates equal to 1 deg/min, temperature dependent ellipticity displays an hysteresis smaller than 5%. However, in order to avoid smearing effects, further data analysis were done only on the rising temperature curves.

From the ellipticity measurements reported in Fig.4, the helix fraction x_h was computed following the relation:

$$x_h(T) = \frac{\theta(T) - \theta(\infty)}{\theta(0) - \theta(\infty)} \quad (2)$$

In Fig.5, x_h is plotted as a function of the reduced temperature T/T^* , where T^* is determined by the intercept of each experimental curve with the $\theta_{1/2}$ value.

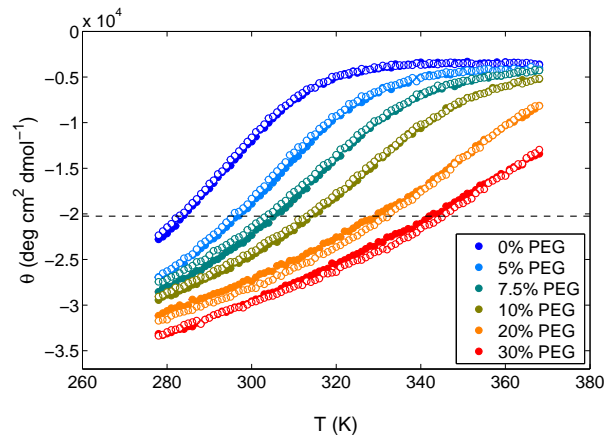


FIG. 4. Ellipticity θ at 222 nm per amino acid of poly(L-glutamic acid) solutions at pH=3.75 vs. temperature for different volume fractions of PEG. Full and open symbols correspond to rising and lowering temperature, respectively. The horizontal line has an ordinate $\theta_{1/2}$ corresponding to the helix fraction $x_h = 1/2$.

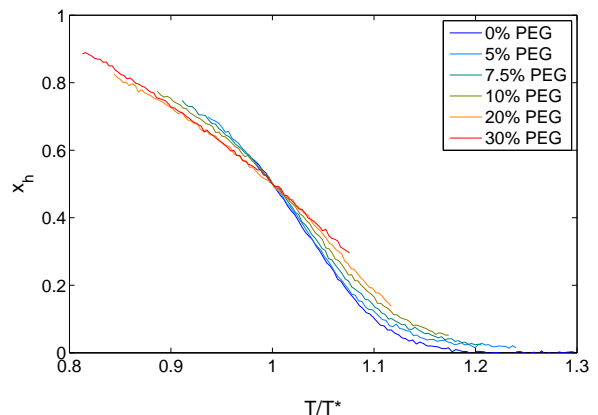


FIG. 5. Helix fraction x_h of poly(L-glutamic acid) solutions at pH=3.75 vs. reduced temperature T/T^* for different volume fractions of PEG.

II. DISCUSSION

Our results will be discussed assuming a two-state transition between coil and helix. This point is not obvious as three states (or more) could be introduced (see e.g. ref.¹³). However, this paper is concerned with the effect of crowding on the transition rather than a detailed analysis of its mechanism. For our purpose the two-state hypothesis is sufficient. Note that in Fig.5 the curves obtained for different PEG volume fractions do not superimpose. Without further analysis this demonstrates that the helix-coil transition cannot be described by the Van't Hoff equation for chemical equilibrium seeing that the latter would imply T/T^* as being a reduced variable.

A. Zimm-Bragg model

The first and simplest model concerned with the helix-coil transition is due to B. H. Zimm and J. K. Bragg⁶. This model is widely used to describe experimental data and a basis of many refinements. In terms of the Zimm-Bragg model, taking the coil state as reference the Gibbs free energy of a given monomer i writes:

$$G_i = -hs_i - Js_i s_{i+1} \quad (3)$$

with $s_i = 0$ or 1 for coil and helix segments, respectively. Here, h corresponds to the free energy cost of a helical nucleus obtained by the formation of one hydrogen bond between i and $i + 4$ monomers:

$$h = H_B - TS_4 \quad (4)$$

where H_B is the bond enthalpy and S_4 the entropy loss resulting from fixing 4 monomers in a helix turn. For charged monomers, H_B is an effective bond enthalpy that accounts also for their electrostatic repulsions. The coupling parameter J accounts for a loss of entropy S_1 that is smaller in the case of adding only one monomer to a pre-existing helix turn. This term is purely entropic and can be written as:

$$J = T(S_4 - S_1) \quad (5)$$

It can be viewed as the free energy cost of the helix extremities. Traditionally, the Zimm-Bragg parameters s and σ are introduced in order to express the statistical weights:

$$\sigma s = e^{h/kT} \quad (6)$$

$$s = e^{(h+J)/kT} = e^{(H_B - TS_1)/kT} \quad (7)$$

corresponding to helix nucleation and propagation, respectively. One gets for σ :

$$\sigma = e^{-J/kT} \quad (8)$$

with kT the thermal energy. Straightforwardly from the above definitions, one can see that s is temperature dependent whereas σ is not. For long chains, as a function of these parameters, the helix fraction x_h and the extent N_h of helical domains (average number of amino acids per helix block) write¹⁴:

$$x_h = \frac{1}{2} + \frac{s - 1}{2((s - 1)^2 + 4\sigma s)^{1/2}} \quad (9)$$

$$N_h = 1 + \frac{2s}{1 - s + ((s - 1)^2 + 4\sigma s)^{1/2}} \quad (10)$$

The fraction $x_h(s)$ displays a sigmoid shape. The slope $(dx_h/ds)_{\frac{1}{2}}$ at the very point $(x_h = 1/2, s = 1)$ of equal helix and coil amounts defines the abruptness of the transition. Eq.9 gives $(dx_h/ds)_{\frac{1}{2}} = 1/4\sigma^{1/2}$.

B. Data analysis

Experimentally, $x_h(T)$ should be more conveniently considered. However due to the primitiveness of the Zimm-Bragg model, direct data fitting using Eq.9 expressed as a function of temperature leads usually to poor results (see for instance ref.¹⁵). In the literature many improvements of the Zimm-Bragg model are proposed (see for instance^{13,16-18}). Alternatively, we focused our data analysis in the near vicinity of the transition temperature and assumed that the Zimm-Bragg model in this narrow temperature range captures the main features of the helix-coil transition. The transition temperature corresponding to $(x_h = 1/2, s = 1)$ writes:

$$T^* = H_B/S_1 \quad (11)$$

Eq.7, 9 and 11 yield:

$$\left(-\frac{dx_h}{d(T/T^*)} \right)_{T=T^*} = \frac{S_1}{k} \times \frac{1}{4\sigma^{1/2}} \quad (12)$$

In practice S_1/k has been measured as being of the order of $1^{19,20}$. This value will be retained in the following. Note that at the transition temperature T^* , the extent of helical domains remains finite and from Eq.10 equal to:

$$N_h(T^*) = 1 + \sigma^{-1/2} \quad (13)$$

Helices being rod-like, their extent allows us to define a correlation length L_h of helical domains:

$$L_h = \frac{1}{2} \times \frac{N_h}{3.6} \times 5.4 \text{ \AA} \quad (14)$$

since the repeat unit of α -helix corresponds to 3.6 residues and 5.4 \AA . Similarly to the notion of persistence length vs. Kuhn length in polymer physics, the factor 1/2 comes from correlations that are symmetrical with respect to an arbitrary origin.

Summary of our results for T^* , σ , N_h and L_h are reported in Table I. For increasing PEG concentration, we observe a systematic variation of the slope of $x_h(T/T^*)$ at T^* (see Fig.5) that corresponds to an increase of the Zimm-Bragg parameter σ and a corresponding decrease of the correlation length L_h of helical domains. Note that the model-dependent values here reported for L_h are in very good agreement with the value directly measured by Muroga et al.²¹ at $\phi_{\text{PEG}} = 0$ by small angle X-ray scattering on poly(L-glutamic acid) at the transition temperature.

C. Variation of the solvent quality

Let us first consider a possible change of the solvent quality due to the increase of PEG concentration, i.e. the co-solute. Such co-solute effect on helix-coil transition has been theoretically studied in ref.²². The authors

TABLE I. Summary of the results obtained by circular dichroism measurements: transition temperature T^* ; Zimm-Bragg parameter σ deduced from the slope at T^* of ellipticity vs. temperature curve; extent N_h and correlation length L_h of helical domains at the transition.

ϕ_{PEG} %	T^* K	σ $\times 10^3$	N_h	L_h Å
0	284	3.45 ± 0.05	18.1 ± 0.1	13.6 ± 0.1
5	297	4.1 ± 0.1	16.6 ± 0.2	12.4 ± 0.2
7.5	305	4.8 ± 0.1	15.4 ± 0.2	11.6 ± 0.2
10	313	6.4 ± 0.2	13.5 ± 0.2	10.4 ± 0.1
20	330	8.3 ± 0.3	12.0 ± 0.2	8.8 ± 0.1
30	342	8.8 ± 0.2	11.6 ± 0.1	8.7 ± 0.1

classify the solvent quality changes into two categories. The first one acts on the Zimm-Bragg parameter s resulting in a shift of the transition temperature (e.g. variation of the pH enters in this category). The second category is concerned with variation of the hydrogen-bonding ability of the solvent due to the co-solute. For instance, one may imagine that the co-solute preferentially binds to helix extremities, lowering their free energy and then increasing the Zimm-Bragg parameter σ but remaining s unaffected. From ref.²², one would expect:

$$\sigma(\phi)^{1/2} = \sigma(0)^{1/2} + e^{-\tilde{J}/kT} \phi \quad (15)$$

where \tilde{J} is the free energy of a helix extremity in contact with the co-solute with a probability $p_{\text{contact}} = \phi$. Naturally, the co-solute may also bind to the helix body (but with a different affinity constant than for the extremities), yielding to a change of the parameter s and a shift of the transition temperature. So that the co-solute should be responsible for effects of both categories. However, a change of the solvent quality with PEG addition should be independent of the chain length and in particular should be observed for small PEG chains. This is not the case. In ref.²³, on the same poly(L-glutamic acid) system but with short PEG chains (400 g/mol), the authors report a stabilization of the helices (as in our experiments), but no change of cooperativity of the transition was reported.

D. Entropic stabilization

The number of possible states for a peptide chain is proportional to the accessible volume that is decreased by a crowding agent. For a given volume fraction ϕ_{PEG} , the entropy of the peptide chain is:

$$S(\phi_{\text{PEG}}) = S(0) + k \ln(1 - \phi_{\text{PEG}}) \quad (16)$$

Considering only entropy variations due to the crowding agent (excluded volume), from Eq.11 the equilibrium

temperature is expected to vary as:

$$\frac{1}{T^*(\phi_{\text{PEG}})} = \frac{1}{T^*(0)} + \frac{k}{H_B} \ln(1 - \phi_{\text{PEG}}) \quad (17)$$

In Fig.6, the reverse transition temperature $1/T^*$ is plotted as a function of $\ln(1 - \phi_{\text{PEG}})$ for the data obtained at pH=3.75. In this figure, the straight lines are guides for the eyes with slopes taken from the literature as equal to $k/H_B = 1/560$ K (i.e. $H_B = 1120$ kcal/mole from ref.²⁴ for fully protonated glutamic acid monomers) and $k/H_B = 1/317$ K (i.e. $H_B = 630$ kcal/mole from ref.²⁵ for fully dissociated glutamic acid monomers), respectively. At least in the regime of low PEG concentration, our results seem in better agreement with the latter value for H_B rather than with the former. At pH=3.75, poly(L-glutamic acid) is certainly not fully but only partly dissociated (the pKa of poly(L-glutamic acid) is of the order of 2.1). Thus, this result may indicate a possible co-solute effect of the first category discussed in the previous section, i.e. PEG co-solute probably lowers the effective hydrogen bond enthalpy H_B .

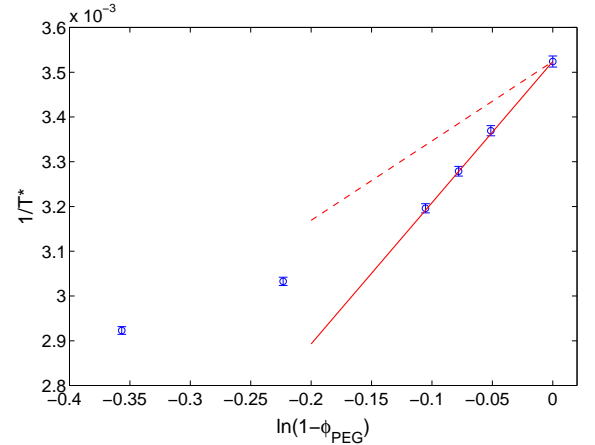


FIG. 6. Reverse transition temperature $1/T^*$ vs. logarithm of the accessible volume fraction $\ln(1 - \phi_{\text{PEG}})$. The straight lines are guides for the eyes with slopes equal to $1/560$ K²⁴ for fully protonated glutamic acid monomers and $1/317$ K²⁵ for fully dissociated glutamic acid monomers, respectively.

From Eq.5, the coupling parameter J (and σ defined by Eq.8) results from a difference of two entropy terms that both are increased by the same quantity with PEG addition (Eq.16). Thus, a simple entropic stabilization mechanism lets us expect that σ is independent of ϕ_{PEG} , which is clearly in disagreement with our finding. Thus, a supplementary mechanism has to be proposed.

E. Polymeric nature of crowding agent

In this paper, we would like to point out the polymeric nature of PEG as crowding agent that has not been considered until now. In our concentration range, long

PEG chains are semi-diluted and form a transient network of characteristic length ξ that can be viewed as a mean distance between two chains. Thus by definition, at length scale below ξ a chain is alone and only interactions between monomers belonging to the same chain are relevant, whereas beyond ξ a monomer experiences interactions with other chains. In good solvent, this yields classically to a swollen conformation of the chain below ξ (monomers of a given chain repeal each other) that becomes gaussian beyond ξ (repulsions are screened due to the presence of other chains)⁹.

In the absence of any peculiar specific interaction between diluted poly(L-glutamic acid) chains and PEG, the formers are fully embedded and participate in the PEG network. Here we suggest that in the same way as local swelling of PEG chains is screened above ξ , the thermodynamics of helices growth should also be influenced by binary contacts with the PEG network. In order to test this picture, we plotted in Fig.7 the average number $N_h(T^*)$ of amino acid per helix at the transition as a function of the ratio of the two lengths $L_h(T^*)/\xi$ in our system. The result strongly suggests two regimes ($L_h(T^*) \ll \xi$ and $\xi \ll L_h(T^*)$ separated by a wide crossover.

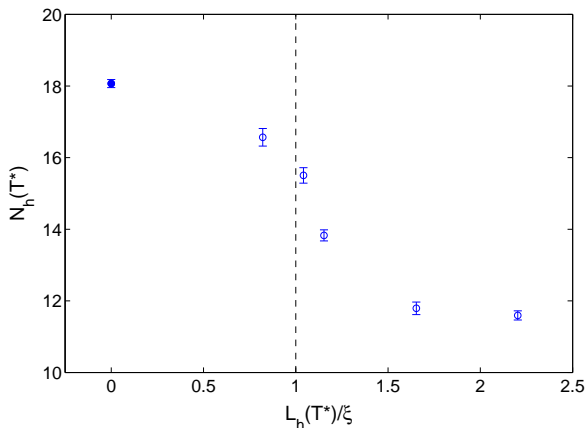


FIG. 7. Average number $N_h(T^*)$ of amino acid per helix at the transition vs. the ratio of the correlation length $L_h(T^*)$ of helices at the transition to the mesh size ξ of the PEG network. The close symbol at $L_h(T^*)/\xi = 0$ corresponds to $\phi_{\text{PEG}} = 0$ (i.e. $\xi \rightarrow \infty$).

Note that in this picture, for a given PEG concentration and for decreasing temperatures, growing helices begin to experience the network at a given temperature such as $L_h = \xi$. So that with PEG, $x_h = f(T)$ cannot be fitted in the entire temperature range with a model (such as the Zimm-Bragg model) that does not introduce the characteristic size of the network.

III. CONCLUSION

We report circular dichroism measurements on the helix-coil transition of poly(L-glutamic acid) in semi-diluted solutions of PEG as a crowding agent that has been fully characterized by small angle neutron scattering. We show that the increase of PEG concentration stabilizes the helices and increases the transition temperature. This point, which has been already reported for other crowding agent species, is in agreement with an "entropic stabilization mechanism". However, we also notice that the increase of crowding agent concentration reduces the mean helix extent at the transition, or in other words reduces its cooperative feature. To our knowledge, this result has not been reported previously and cannot be accounted for by an entropic stabilization. Comparing the two lengths of the system, i.e. mean length of helices at the transition and mesh size of PEG network, our results strongly suggest two regimes: helices shorter or longer than the mesh size, each regime having its own value for the Zimm-Bragg parameter σ that characterizes the cooperativity of the transition. Until now, these kinds of effect have not been considered from a theoretical point of view and we hope that our measurements will contribute to stimulate works in this direction.

- ¹A. P. Minton, "The effect of volume occupancy upon the thermodynamic activity of proteins: some biochemical consequences," *Molecular and Cellular Biochemistry*, **55**, 119 (1983).
- ²H.-X. Z. G. Rivas and A. Minton, "Macromolecular crowding and confinement: Biochemical, biophysical, and potential physiological consequences," *Annu. Rev. Biophys.*, **37**, 375 (2008).
- ³G. Ziv, G. Haran, and D. Thirumalai, "Ribosome exit tunnel can entropically stabilize α -helices," *PNAS*, **102**, 18956 (2005).
- ⁴L. Javidpour and M. Sahimi, "Confinement in nanopores can destabilize alpha-helix folding proteins and stabilize the beta structures," *J. Chem. Phys.*, **135**, 125101 (2011).
- ⁵A. Kudlay, M. S. Cheung, and D. Thirumalai, "Crowding effects on the structural transitions in a flexible helical homopolymer," *Phys. Rev. Lett.*, **102** (2009).
- ⁶B. H. Zimm and J. K. Bragg, "Theory of the phase transition between helix and random coil in polypeptide chains," *J. Chem. Phys.*, **31**, 526 (1959).
- ⁷A. Badasyan, A. Giacometti, Y. Mamasakhlisov, V. F. Morozov, and A. Benight, "Microscopic formulation of the Zimm-Bragg model for the helix-coil transition," *Phys. Rev. E*, **81**, 021921 (2010).
- ⁸A. Brûlet, D. Lairez, A. Lapp, and J.-P. Cotton, "Improvement of data treatment in small angle neutron scattering," *J. Appl. Cryst.*, **40**, 165 (2007).
- ⁹P. G. de Gennes, *Scaling concepts in polymer physics*. (Cornell Univ. Press, Ithaca, 1996).
- ¹⁰J. E. Mark and P. J. Flory, "The configuration of the polyoxyethylene chain," *J. Am. Chem. Soc.*, **87**, 1415 (1965).
- ¹¹J. Su, R. Hodges, and C. Kay, "Effect of chain length on the formation and stability of synthetic α -helical coiled coils," *Biochemistry*, **33**, 15501 (1994).
- ¹²H. Nakamura and A. Wada, "Dielectric studies of aqueous solutions of poly(L-glutamic acid)," *Biopolymers*, **20**, 2567 (1981).
- ¹³S. Lifson and A. Roig, "On the theory of helix-coil transition in polypeptides," *J. Chem. Phys.*, **34**, 1963 (1961).
- ¹⁴A. Grosberg and A. Khokhlov, *Statistical physics of macromolecules* (AIP Press, New York, 1994).
- ¹⁵R. L. Baldwin, " α -helix formation by peptides of defined sequence," *Biophys. Chem.*, **55**, 127 (1995).

- ¹⁶Y. Chen, Y. Zhou, and J. Ding, "The helix-coil transition revisited," *Proteins* (2007).
- ¹⁷O. K. Vorov, D. R. Livesay, and D. J. Jacobs, "Helix/coil nucleation: A local response to global demands," *Biophys. J.*, **97**, 3000 (2009).
- ¹⁸A. Murza and J. Kubelka, "Beyond the nearest-neighbor zimm-bragg model for helix-coil transition in peptides," *Biopolymers*, **91**, 120 (2009).
- ¹⁹Z. Shi, C. A. Olson, G. D. Rose, R. L. Baldwin, and N. R. Kallenbach, "Polyproline ii structure in a sequence of seven alanine residues," *PNAS*, **99**, 9190 (2002).
- ²⁰Y. Z. Ohkubo and C. L. Brooks, "Exploring flory's isolated-pair hypothesis: Statistical mechanics of helix-coil transitions in polyalanine and the c-peptide from rnase a," *PNAS*, **100**, 13916 (2003).
- ²¹Y. Muroga, H. Tagawa, Y. Hiragi, T. Ueki, M. Kataoka, Y. Izumi, and Y. Amemiya, "Conformational analysis of broken rod-like chains. 2. conformational analysis of poly(d-glutamic acid) in aqueous solution by small-angle x-ray scattering," *Macromolecules*, **21**, 2756 (1988).
- ²²O. Farago and P. Pincus, "Solute effects on the helix-coil transition," *Eur. Phys. J. E*, **8**, 393 (2002).
- ²³C. B. Stanley and H. H. Strey, "Osmotically Induced Helix-Coil Transition in Poly(Glutamic Acid)," *Biophys. J.*, **94**, 4427 (2008).
- ²⁴J. Hermans, "Experimental free energy and enthalpy of formation of the α -helix," *J. Phys. Chem.*, **70**, 510 (1966).
- ²⁵J. Rifkind and J. Applequist, "The helix interruption constant for poly-l-glutamic acid from the pressure dependence of optical rotation," *J. Am. Chem. Soc.*, **86**, 4207 (1964).